Time-frequency approach to relativistic correlations in quantum field theory

Benjamin Roussel[*] and Alexandre Feller[†]
Advanced Concepts Team, European Space Agency, Noordwijk, 2201 AZ, The Netherlands

(Received 6 June 2019; published 16 August 2019)

Moving detectors in relativistic quantum field theories reveal the fundamental entangled structure of the vacuum, which manifests, for instance, through its thermal character when probed by a uniformly accelerated detector. In this paper, we propose a general formalism inspired from both signal processing and correlation functions of quantum optics to analyze the response of pointlike detectors following a generic, nonstationary trajectory. In this context, the Wigner representation of the first-order correlation of the quantum field is a natural time-frequency tool to understand single-detection events. This framework offers a synthetic perspective on the problem of detection in relativistic theory and allows us to analyze various nonstationary situations (adiabatic, periodic) and how excitations and superpositions are deformed by motion. It opens up an interesting perspective on the issue of the definition of particles.

DOI: 10.1103/PhysRevD.100.045016

I. INTRODUCTION

One of the fundamental differences between relativistic quantum field theories and quantum mechanics is the deeply entangled structure of quantum fields. While this can be understood in a general formal setting [1,2], one of the clearest phenomena illustrating this is the entangled structure of the vacuum state, which is revealed by its thermal character in curved spacetime [3] or by a uniformly accelerated observer [4], known as the Hawking and Unruh effects, respectively.

The correlated nature of the vacuum is nicely probed by considering a moving detector in spacetime coupled to the quantum field. Such models are known as Unruh-Dewitt detectors. The thermal nature of the vacuum is then seen through its photodetection response. Many questions can then be addressed, such as the role of causality [5], the behavior under different motions [6–8], or the effect of the switching function of the detector [9,10]. A similar photodetection approach has been used in quantum optics since the work of Glauber on coherence functions [11,12] and has been extended to condensed matter situations [13].

However, the interpretation of these responses in the context of relativistic quantum field theory in flat or in curved spacetime is subtler than in quantum optics, since no general notion of particles can be defined in the standard way. The qualitative reason comes from the nonexistence of a global definition of time. Two directions can then be taken. The first direction is to have an operational perspective: particles are defined through the response signal of the detector itself [4]. The second direction follows a more pragmatic interpretation of the detector's response: the detector is simply seen as a "fluctuometer," as a system that responds to the fluctuations of the quantum field. The signal should not *a priori* be interpreted as coming from a particle content [6,14,15].

Following this latter point of view is similar to adopting a signal processing perspective, which we will adopt here. In a nonstationary context, physically meaningful information can be extracted from the signal by performing a time-frequency analysis, giving us access to the evolution in time of the frequency content of the response. Time-frequency (or timescale) analysis is now a major tool in signal processing, especially the Wigner function distribution [16]. Historically, the Wigner function has been introduced in quantum mechanics as a phase-space representation of the quantum state [17]. This distribution is now widely used in quantum optics [18] and has been recently adapted to analyze coherence properties of electrons in the quantum Hall regime [19,20].

In this paper, we present a unified view on the response of a moving detector probing a relativistic quantum field using a time-frequency approach to the correlation functions of the field based on the Wigner distribution. The main goal is to introduce good framework to analyze the response of a detector in general situations where the state of the field can contain excitations, for an arbitrary trajectory. This is achieved by using both the correlation function formalism and a time-frequency analysis. Physically realistic situations can then be analyzed quantitatively through analytical and numerical computations. Having a time-frequency analysis and a quantum optics perspective on the problem of relativistic detector response provides a synthetic approach to the problem of moving detectors. Besides, this time-frequency perspective sheds

[*]benjamin.roussel@esa.int
[†]alexandre.feller@esa.int

new light on the interpretation of the measured signal and the problem of defining a notion of particles. Indeed, having two natural ways of defining particles, the standard many-body one and the operational one, demands that we relate them and understand their interplay. Time-frequency analysis offers a way to define relative stationary timescales from which notions of particles can be defined locally in spacetime and frequency domains.

This paper is structured as follows: In Sec. II, we set up the general framework of correlation functions and their time-frequency representation through the Wigner function. In Sec. III, we analyze the response of a detector probing the vacuum for different nonstationary motions of the detector. We give a detailed analysis of the adiabatic regime, its corrections, and its breakdown. Section IV is dedicated to the study of the detector's response in the presence of excitations in the uniformly accelerated and realistic motions. In particular, it addresses how coherences in a superposition transform can be analyzed straightforwardly. We conclude this paper in Sec. V by discussing how different notions of particles can be defined from the signal from a time-frequency analysis.

II. FIRST-ORDER CORRELATION

A. Context and photodetection

Systems in quantum optics, condensed matter, and high-energy physics are well described using the framework of quantum field theories. In this context, the experimentally relevant quantities are not the fields themselves but correlation functions constructed from them. Some of them are known in quantum optics as coherence or Glauber functions. They naturally come up when analyzing the photodetection response.

We are also interested in the photodetection response of a system moving arbitrarily in flat spacetime. It is designed to detect a single excitation of a relativistic quantum field. We suppose that this device is moving in Minkowski spacetime with a given trajectory $\mathbf{x}(\tau)$ and is coupled linearly to a massless scalar field $\phi(x)$. In the inertial laboratory reference frame, the Hamiltonian is given in the interaction picture by

$$H_I(\tau) = d(\tau) \cdot \phi^{(I)}(t(\tau), \mathbf{x}(\tau)). \tag{1}$$

If we model the detector as a two-level system of energy ω_{eg}, then $d(\tau) = -g\sigma_x(\tau)$, with g being the coupling constant.

We are now interested in the probability to measure the excited state after a time τ. Since the coupling is weak, we can use time-dependent perturbation theory, expand the evolution operator at the first order, and obtain the desired probability $p_{\omega_{eg}}(\tau)$:

$$p_{\omega_{eg}}(\tau) = \left(\frac{g}{\hbar}\right)^2 \int_0^\tau e^{i\omega_{eg}(\tau_1-\tau_2)} G(\tau_1, \tau_2) \mathrm{d}\tau_1 \mathrm{d}\tau_2. \tag{2}$$

The function $G(\tau_1, \tau_2)$ depends only on the state of the scalar field and is defined as a first-order correlation function:

$$G_\rho(\tau_2, \tau_1) = \mathrm{tr}(\phi^{(I)}(t(\tau_1), \mathbf{x}(\tau_1))\phi^{(I)}(t(\tau_2), \mathbf{x}(\tau_2))\rho). \tag{3}$$

This correlation function contains all of the contribution of the field to first order in the photodetecting signal. There is, however, a major difference between this signal and the standard one found by Glauber in quantum optics. Indeed, for photons, we have $G^{\mathrm{ph}}_\rho(\tau_2, \tau_1) = \mathrm{tr}(E^-(\tau_1)E^+(\tau_2)\rho)$, where $E^\pm$ are the positive- and negative-frequency parts of the electric field operator. In the relativistic regime, the correlation function does not depend on only the product $\phi^-\phi^+$ but on the full field, as in Eq. (3) [21]. One reason behind this difference is fundamental and comes from the fact that the definition of positive and negative frequencies depends on the time coordinate. For a detector in a general trajectory or in the presence of a gravitational field, there is no global definition of the time coordinate, and so there is no general decomposition of the field in momentum space. The notions of excitation and of vacuum become relative concepts.

Equation (2) can be generalized by introducing a generic linear response function $\chi(\tau_2, \tau_1)$ of the detector, and the resulting photodetection signal is then obtained by

$$p(\tau) = \int_{\mathbb{R}} \chi_\tau(\tau_2, \tau_1) G(\tau_1, \tau_2) \mathrm{d}\tau_1 \mathrm{d}\tau_2. \tag{4}$$

The function $\chi_\tau(\tau_2, \tau_1)$ characterizes the response of the detector, and its form depends on the type of detector we use. The photodetection probability is then just the scalar product between this response function and the first-order correlation function. For a broadband device, the response will be local in time with $\chi(\tau_2, \tau_1) = f(\tau)\delta(\tau_2 - \tau_1)$ and $f(\tau)$ being the switching function. On the contrary, for a narrow-band device like the two-level system, we measure the Fourier transform of the correlation function.

B. Definitions

1. First-order and excess correlations

The photodetection problem shows that the quantity encoding the response of pointlike detector at first order is given by a first-order correlation function of the field defined as

$$G_\rho(\tau_2, \tau_1) = \mathrm{tr}(\phi(\tau_1)\phi(\tau_2)\rho) = \langle \phi(\tau_1)\phi(\tau_2)\rangle_\rho, \tag{5}$$

with the notation $\phi(\tau) = \phi^{(I)}(t(\tau), \mathbf{x}(\tau))$ for a given trajectory $x(\tau)$. Depending on the context, this function and all the higher-order ones that could be defined are called correlation functions or Wightman's functions. In quantum optics, the term *coherence functions* is used but

involves correlation functions of the positive- and negative-frequency parts of the field. We will stick to the general quantum field theory denomination of correlation functions. From now on, we use a unit system in which $\hbar = c = 1$ and the Minkowski metric signature $(-,+,+,+)$.

The most important situation occurs when the vacuum state of the field is prepared. The correlation function can be computed exactly and is given by

$$G_{|0\rangle}(\tau_2,\tau_1) = \frac{1}{4\pi^2}\frac{1}{-(t(\tau_1)-t(\tau_2)+i\epsilon)^2+(\mathbf{x}(\tau_1)-\mathbf{x}(\tau_2))^2}, \tag{6}$$

where, for the moment, we use the standard regularization of $i\epsilon$. The question of regularization will be discussed in more detail in the next section.

Let us now add an extra excitation in a normalized wave packet Φ:

$$\phi[\Phi]|0\rangle = \int_{\mathbb{R}^3} \Phi(t,\mathbf{x})\phi^\dagger(t,\mathbf{x})|0\rangle \mathrm{d}^3x. \tag{7}$$

By Wick's theorem, and using the notation $\Phi^*(\mathbf{x}(\tau), t(\tau)) = \Phi(\tau)$, the first-order correlation now reads

$$\begin{aligned} G_{\phi[\Phi]|0\rangle}(\tau_2,\tau_1) = {} & G_{|0\rangle}(\tau_2,\tau_1) + \Phi^*(\tau_1)\Phi(\tau_2) \\ & + \Phi(\tau_1)\Phi(\tau_2) + \mathrm{H.c.} \end{aligned} \tag{8}$$

This suggests that we decompose the correlation function into two parts by the equation

$$G_\rho(\tau_2,\tau_1) = G_{|0\rangle}(\tau_2,\tau_1) + \Delta G_\rho(\tau_2,\tau_1). \tag{9}$$

The interpretation is intuitively clear in the pure-state case described by Eq. (8), since we can clearly think of excitations over the vacuum. For a general density matrix, the decomposition in Eq. (9) comes from the fact that a measurement must be understood as a comparison between the state of the field and a reference state, which in this case is the vacuum. This choice is also justified by the fact that a reasonable physical state will have the same behavior as the vacuum at high energy, for both absorption and emission processes. This turns out to be important for the regularization aspects, as we will see. However, such a decomposition might be more subtle when taking into account general relativity and backreaction effects.

In the following, Sec. III will focus on the vacuum contribution, while Sec. IV will be dedicated to the study of different kinds of excitation.

2. On regularization

In quantum field theory, the correlation functions are actually not proper functions but Lorentz-invariant distributions on spacetime [22]. The distribution character comes from the necessary divergences of the correlation functions, which need to be properly regularized.

The standard $-i\epsilon$ regularization procedure, that was used for instance in Eq. (6), corresponds to an ultraviolet cutoff for the detector. However, in a general reference frame, the frequency content is redistributed, and some care must be taken to ensure the proper regularization. A natural choice is to perform a high-energy cutoff regularization similar to the $-i\epsilon$ regularization of the modes in the proper reference frame of the detector [23].

This turns out to be equivalent to spatial regularizations, with spatially extended detectors [5,9,24,25] that were introduced to solve the issues encountered with causality, leading to the impossibility to recover the Unruh effect with a causal detector [5], under the standard regularization scheme.

All of these regularization procedures are equivalent and lead to well-defined Lorentz-invariant and causal correlation functions. They amount to subtracting the vacuum contribution found by an inertial detector [24]. In the end, this strategy matches the one used in quantum optics and condensed matter. The rationale behind it is physically intuitive, because the correlator itself is not probed directly, but is always compared to that of a reference state, as defined in Eq. (9).

C. Representations of the first-order correlation

1. Time and frequency representations

The time representation $G_\rho(\tau_2,\tau_1)$ is the natural representation to use to look for dynamical information. The diagonal $G_\rho(\tau,\tau)$ corresponds to an energy density per unit time, while the off-diagonal elements, which are complex numbers, give the coherences in time. However, this representation is not well suited to understanding the kind of processes happening in the detection events, since they are encoded in the τ_1-τ_2 dependence of the phase of $G_\rho(\tau_2,\tau_1)$.

This is solved by going to the frequency domain. By computing a double Fourier transform, we can then define

$$\begin{aligned} G_\rho(\omega_2,\omega_1) &= \int_{\mathbb{R}^2} G_\rho(\tau_2,\tau_1) e^{i(\omega_1\tau_1-\omega_2\tau_2)} \mathrm{d}\tau_1 \mathrm{d}\tau_2 \\ &= \langle \phi^\dagger(\omega_1)\phi(\omega_2)\rangle_\rho, \end{aligned} \tag{10}$$

where the field $\phi(\omega)$ is defined with respect to an inertial mode decomposition as

$$\phi(\omega) = \int_{\mathbb{R}^3} (a_{\mathbf{k}} f^*_{\mathbf{k}}(\omega) + a^\dagger_{\mathbf{k}} f_{\mathbf{k}}(-\omega)) \frac{\mathrm{d}^3\mathbf{k}}{2\omega_{\mathbf{k}}(2\pi)^3}, \tag{11}$$

with

$$f^*_{\mathbf{k}}(\omega) = \int_{\mathbb{R}} e^{ik\cdot x(\tau)} e^{i\omega\tau} \mathrm{d}\tau. \tag{12}$$

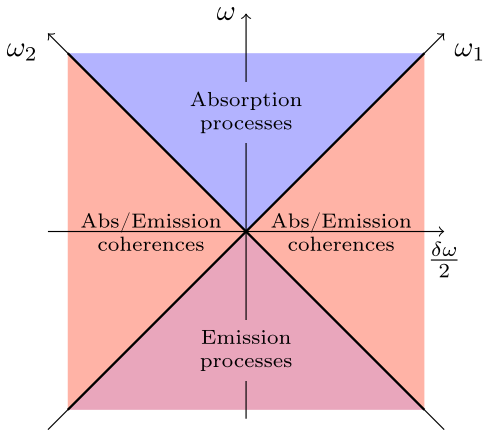

FIG. 1. Decomposition of the Fourier plane into four quadrants: the upper quadrant corresponds to absorption processes, the lower quadrant to emission processes, and the side quadrants to the coherences between emission and absorption processes. While this particle-like interpretation makes sense for inertial observers, it does not necessarily hold as such for any trajectory.

The Fourier plane (ω_1, ω_2) is traditionally divided into four quadrants, as shown in Fig. 1. The positive-frequency quadrant, defined by $\omega_1 > 0$ and $\omega_2 > 0$, corresponds to the absorption processes, while the negative-frequency quadrant corresponds to the emission processes. Finally, the two quadrants defined by $\omega_1\omega_2 < 0$ correspond to the coherences between emission and absorption processes. This interpretation follows the operational definition of particles and matches the many-body one for inertial detectors. This equivalence does not hold for a general moving detector, since nothing guaranties that the same notion of particles exists in all frames. Still, we can expect that the different notions of particles that could be defined should match at sufficiently high frequency (compared to acceleration or local curvature). This is corroborated for a uniformly accelerated detector: the inertial modes $u^{(i)}_\omega$ and the accelerated modes $u^{(a)}_\omega$ are related by a Bogoliubov transformation $u^{(a)}_\omega = (u^{(i)}_k - e^{-\pi\omega/a}\bar{u}^{(i)}_k)/\sqrt{1-e^{-2\pi\omega/a}}$, from which we clearly see that for $\omega \gg a$, $u^{(a)}_\omega \approx u^{(i)}_k$. This remark suggests that instead of trying to define a global notion of particles, we should maybe seek to define local notions of particles relative to the different scales of the problem: this hints toward a time-frequency definition of particles, an idea that will be discussed in more detail in Sec. V.

The diagonal $G_\rho(\omega,\omega)$ corresponds to the excitation occupation number per frequency. A convenient representation of the Fourier plane, also shown in Fig. 1, is given by the variables $\delta\omega = \omega_1 - \omega_2$ and $\omega = (\omega_1+\omega_2)/2$, conjugated to $\tau_1 - \tau_2$ and $(\tau_1+\tau_2)/2$, respectively, which, as we will see, are the natural variables for the time-frequency Wigner representation.

The frequency domain representation has complementary advantages compared to the time representation. When analyzing the response of a detector in a stationary trajectory, choosing one representation over the other is a matter of convenience. However, most physically realizable motions are not stationary, and a time-frequency representation is called for. Such representations exist and have been analyzed in depth in signal processing research [16]. The common one used in physics is the Wigner representation, which we will discuss in the context of relativistic field theory.

2. Time-frequency representation

The time and frequency representations have complementary properties: while one clearly represents the time evolution, the other clearly shows the type of processes taking place. While this is not a major issue for stationary signals, it becomes one for nonstationary signals like those obtained by a detector moving in a general trajectory. Fortunately, it is possible to have the best of both worlds in one clear time-frequency representation. We propose to analyze the Wigner representation of the correlation function defined as

$$W_\rho(\tau,\omega) = \int_{\mathbb{R}} G_\rho(\tau+\upsilon/2, \tau-\upsilon/2)e^{i\omega\upsilon}\mathrm{d}\upsilon. \quad (13)$$

In the same way as Eq. (9), we can define an excess Wigner function ΔW_ρ with respect to the vacuum:

$$W_\rho(\tau,\omega) = W_{|0\rangle}(\tau,\omega) + \Delta W_\rho(\tau,\omega). \quad (14)$$

This vacuum Wigner function must be regularized. As argued in Sec. II B 2, this is done by properly analyzing the response in the vacuum of an inertial detector and subtracting it. The Wigner function $W_{|0\rangle}$ is again decomposed into two contributions:

$$W_{|0\rangle}(\tau,\omega) = W^{\mathrm{in}}_{|0\rangle}(\tau,\omega) + \Delta_{\mathrm{in}}W_{|0\rangle}(\tau,\omega). \quad (15)$$

The first one, $W^{\mathrm{in}}_{|0\rangle}$, is the divergent inertial contribution which can be evaluated easily as $W^{\mathrm{in}}_{|0\rangle} = \frac{|\omega|}{2\pi}\Theta(-\omega)$. The second, $\Delta_{\mathrm{in}}W_{|0\rangle}$, is the regular part that encodes the noninertial contributions. It is a Fourier transform of Eq. (6) (without the $i\epsilon$ regularization) defined by

$$\Delta_{\mathrm{in}}W_{|0\rangle}(\tau,\omega) = \frac{1}{4\pi^2}\int_{\mathbb{R}}\left(\frac{1}{(\Delta x(\tau,\upsilon))^2} - \frac{1}{-\tau^2}\right)e^{i\omega\upsilon}\mathrm{d}\upsilon, \quad (16)$$

with $\Delta x(\tau,\upsilon) = x(\tau+\upsilon/2) - x(\tau-\upsilon/2)$.

The simplest situation is, of course, to consider an inertial detector in the vacuum. The response of the detector will then be given by $W(\tau,\omega) = \frac{|\omega|}{2\pi}\Theta(-\omega)$. This Wigner function is independent of τ, which is a natural

consequence of the stationary character of the trajectory. Its form could have been anticipated by remembering Fermi's golden rule, which states that the transition rate is given to first order by $2\pi d(\omega)f(\omega)$, with $d(\omega)$ being the density of states and $f(\omega)$ their distribution, both in energy space. For our relativistic setup, the relativistic density of state is given by $\mathrm{d}^3k/2k^0(2\pi)^3 = \omega \mathrm{d}\omega/4\pi^2$, since in the massless case $\omega = |\mathbf{k}|$.

Nontrivial physics is unraveled for a detector in a uniformly accelerated motion. Indeed, consider the trajectory to be $x(\tau) = (a^{-1}\sinh(a\tau), a^{-1}(\cosh(a\tau) - 1))$. Then the now well-known thermal response is obtained:

$$\Delta_{\mathrm{in}} W_{|0\rangle}(\tau,\omega) = \frac{\omega}{2\pi}\frac{1}{e^{2\pi\omega/a} - 1}. \tag{17}$$

While still stationary as expected, the Wigner function does not vanish for positive omega. This comes from the mixing of positive and negative frequencies between the inertial and uniformly accelerated modes. The response of the detector is the same as a thermal state with a temperature given by (again using the SI units)

$$T = \frac{\hbar}{ck_B}\frac{a}{2\pi}. \tag{18}$$

The Wigner function possesses a nice set of properties. First, for a stationary signal like the previous examples, the Wigner function is time independent and positive. Moreover, the Wigner function possesses a frequency symmetry $W(\tau,\omega) = W(\tau,-\omega)$ coming from the Hermitian property of the field. Second, its marginals give access to the probability distribution of the conjugated variable. For instance, averaging over time gives the spectral energy density distribution

$$f(\omega) = \overline{W(t,\omega)}^t. \tag{19}$$

In the T-periodic case, this average is taken over a time period, implying $f(\omega) = \frac{1}{T}\int_{-T/2}^{T/2} W(\tau,\omega)\mathrm{d}\tau$. Similarly, the integration over frequency gives the power $P(\tau)$, which is finite only for the regularized Wigner function:

$$P(\tau) = \int \Delta_{\mathrm{in}} W_\rho(\tau,\omega)\frac{\mathrm{d}\omega}{2\pi} = \Delta_{\mathrm{in}} G_\rho(\tau,\tau). \tag{20}$$

This quantity has an interesting relation to the trajectory of the detector in the one-dimensional case, as we will see later, and it was proposed to use it as a general definition of temperature in curved spacetime [26,27]. Finally, the average over time and positive frequency gives back the average energy measured by the detector:

$$\langle E\rangle_\rho = \int_{\mathbb{R}\times[0,+\infty[} \Delta_{\mathrm{in}} W_\rho(\tau,\omega)\mathrm{d}\tau\frac{\mathrm{d}\omega}{2\pi}, \tag{21}$$

an important property to keep in mind to normalize the states we will consider.

3. On causality

Many different kinds of time-frequency representations exist and have been analyzed in the signal processing literature [16]. They can be classified according to a set of natural properties we could demand for a good representation of physical processes: unitarity (a measurement result translates as a scalar product for representations), marginals corresponding to spectral density and power spectrum, positivity (negativity prevents probabilistic interpretations), linearity (a linear filter translates as a linear filter for the representations), causality, and time-reversal symmetry. However, it happens that it is not possible to construct a function satisfying all those requirements. Table I shows the properties of two important time-frequency distributions.

Up to now, in the context of pointlike detectors probing a relativistic quantum field, only the Page distribution, which is a causal time-frequency distribution, has been studied [5,9,24]. Indeed, the main motivation was to understand if the thermal behavior would appear in a causal response, which is not how the standard Unruh effect is derived.

While this is more natural, the Page distribution is not convincingly more physical than a noncausal one, since we still integrate over the whole past history of the motion. Indeed, a true physical response is causal and happens during a finite duration. This is properly modeled by considering a causal switching function $\chi_\tau(\tau_2,\tau_1)$ with finite support. By putting causality considerations in the switching function, focusing on the Page distribution is not mandatory anymore. It is even more interesting to consider the Wigner distribution, containing the same information as the Page one, since it has a clearer interpretation. First, time-reversal symmetry in the physical processes will be properly represented by the Wigner distribution. Moreover, the Wigner function possesses the linearity property, which means that the Wigner transform of a linearly filtered signal is simply the scalar product between the Wigner functions of the filter and the original signal. This is a clear advantage over the other distribution for both signal processing tasks and interferometric experiments.

TABLE I. Comparison of the properties of the Page and Wigner distributions.

Properties	Wigner	Page
Unitarity	✓	✓
Positivity	✗	✗
Marginals	✓	✓
Linearity	✓	✗
Causality	✗	✓
Time reversal	✓	✗

III. A DETECTOR IN THE VACUUM

Let us now discuss the response of a detector probing the inertial vacuum. The main purpose here is to understand the structure of the Wigner function of the vacuum for a generic trajectory. After setting up the framework, we will first analyze the slow deviations from the uniformly accelerated case corresponding to the adiabatic approximation. We will then discuss its breakdown by analyzing oscillatory motions in the vacuum to finish with more physically realizable motions.

A. General (1+1)D motion

To simplify the theoretical analysis, we will consider here a $(1+1)$D generic motion. The solution of the special relativistic equations of motion for a detector can be parametrized in a transparent way. Starting from the normalization condition on the four-velocity $-u_t^2+u_x^2=-1$, we have the natural parametrization:

$$\mathbf{u}(\tau)=\begin{pmatrix}\cosh A(\tau)\\ \sinh A(\tau)\end{pmatrix}. \tag{22}$$

By denoting $a(\tau)$ the oriented norm of the four-acceleration $a^\mu(\tau)$ (positive if the acceleration goes towards $x>0$, negative otherwise) and reinjecting into the equation for the four-acceleration, we find that $a^2=(\partial_\tau A)^2$ and, in the locally inertial frame at $\tau=0$, we have

$$\mathbf{x}(\tau)=\begin{pmatrix}\int_0^\tau \cosh A(\tau')\mathrm{d}\tau'\\ \int_0^\tau \sinh A(\tau')\mathrm{d}\tau'\end{pmatrix}, \tag{23}$$

where $A(\tau)=\int_0^\tau a(\tau')\mathrm{d}\tau'$. From this, we can go one step further and express $\Delta x^2(\tau+\upsilon/2,\tau-\upsilon/2)$ in a suitable form for analytical and numerical analysis. For that, we introduce the quantity

$$A_\tau(\upsilon)=\int_\tau^{\tau+\upsilon} a(\tau')\mathrm{d}\tau'=A(\tau+\upsilon)-A(\tau). \tag{24}$$

We then have

$$\Delta x^2(\tau+\upsilon/2,\tau-\upsilon/2)=-\int_{-\tau/2}^{\tau/2}\cosh(A_\tau(\tau_1)-A_\tau(\tau_2))\mathrm{d}\tau_1\mathrm{d}\tau_2. \tag{25}$$

Using the cosh definition, we can see that this double integral can be reexpressed as a product of two simple ones:

$$\Delta x^2(\tau+\upsilon/2,\tau-\upsilon/2)=-f_+(\tau,\upsilon)f_-(\tau,\upsilon), \tag{26}$$

where $f_\pm(\tau,\upsilon)=\int_{-\upsilon/2}^{\upsilon/2}\exp(\pm A_\tau(\upsilon'))\mathrm{d}\upsilon'$. We can also reexpress the trajectory in terms of $f_\pm$. A description in the locally inertial frame at time τ would simply be

$$\Delta\mathbf{x}_\tau(\upsilon)=\frac{1}{2}\begin{pmatrix}f_+(\tau,\upsilon)+f_-(\tau,\upsilon)\\ f_+(\tau,\upsilon)-f_-(\tau,\upsilon)\end{pmatrix}. \tag{27}$$

This expression in terms of $f_\pm$ possesses a few advantages. It is centered around τ, which allows us to perform expansion for small values of υ. Conversely, it allows precise numerical evaluation around small υ values, which is of prime importance in the regularization scheme we have chosen.

The Wigner function can then be computed using Eq. (16). An interesting property can already be obtained for the power $P(\tau)$. Indeed, by computing the two sides of Eq. (20), we have

$$P(\tau)=\frac{1}{4\pi^2}\frac{a_\tau^2}{12}. \tag{28}$$

The rationale behind defining local temperature in a general spacetime [26,27] comes from this relation and the fact that the acceleration for a uniformly accelerated detector is proportional to the temperature [Eq. (18)], a property that remains true for an adiabatic motion, as we will now see.

B. Adiabatic regime and its breakdown

1. Adiabatic regime

When acceleration changes slowly, we expect the Wigner function to be close to the uniformly accelerated case: this is called the adiabatic regime [7,25,28,29]. More precisely, we expect the main contribution to the Wigner function to be similar to a thermal response with a time-dependent temperature $T(\tau)$ proportional to the instantaneous acceleration $a(\tau)$.

For the purpose of this discussion, we write explicitly the functional dependence on the acceleration of the Wigner function as $W[a(\tau)](\tau,\omega)$. Given a time τ, we denote the uniformly accelerated trajectory having the acceleration $a(\tau)$ by a_τ. Doing an expansion around this trajectory, we obtain

$$W[a(\tau)]=W[a_\tau]+\int_{\mathbb{R}}\frac{\delta W}{\delta a(\upsilon)}[a_\tau]\delta a(\upsilon)\mathrm{d}\upsilon+\frac{1}{2}\int_{\mathbb{R}^2}\frac{\delta^2 W}{\delta a(\upsilon_1)\delta a(\upsilon_2)}[a_\tau]\delta a(\upsilon_1)\delta a(\upsilon_2)\mathrm{d}\upsilon_1\mathrm{d}\upsilon_2. \tag{29}$$

The first term corresponds to the adiabatic response of the detector: the Wigner function is the thermal distribution with a time-dependent temperature proportional to the instantaneous acceleration a_τ. The other terms are corrections to this dominant term.

This development is meaningful when the variations of the acceleration $\delta a_\tau(\upsilon)$ around a given time τ are small compared to the acceleration a_τ over a timescale $\tau_s\gg a_\tau^{-1}$:

$$\delta a_\tau(\upsilon)\ll a_\tau \quad \text{with} \quad \upsilon\le\tau_s. \tag{30}$$

The timescale τ_s, that we could call adiabatic or stationary time, is of prime importance, since it gives us the interval of time around τ over which we can consider the motion uniformly accelerated. Moreover, the variation $\delta a_\tau(v)$ can itself be seen as a function of the derivative $(\dot{a}, \ddot{a}, \ldots)$. In good regimes, it is legitimate to perform an expansion in these derivatives and obtain the reduced and more familiar criterion $\dot{a}/a^2 \ll 1$.

Thus, both the amplitude and the frequency of the perturbation play a role in defining the adiabatic regime and deviations from it. To properly understand the different regimes of the response, we consider an oscillatory acceleration of the form $a(\tau) = a_0 + a_1 \sin(2\pi f \tau)$ with a_0 a constant acceleration, with (a_1, f) being the amplitude and frequency of the oscillatory drive [8]. The functional expansion of Eq. (29) can then qualitatively be seen as an expansion in a_1/a_0, while the derivative expansion of δa is an expansion in $(2\pi f)/a_0$. The different regimes can then be classified as follows:

(1) The adiabatic regime is valid when the perturbation is small, such that $a_1 \ll a_0$ and $2\pi f \ll a_0$. The thermal response follows the acceleration as in $W[a_\tau]$ and is corrected by small terms in the derivatives of the acceleration.
(2) The adiabatic regime *per se* breaks down when one of the two conditions above is not fulfilled and will be analyzed in the next section. In the regime $a_1 \ll a_0$ and $f \gtrsim a_0$, the functional expansion still works, but the terms rearrange themselves such that a thermal response is still present at the average acceleration $\bar{a} = a_0$ plus corrections of order $1/f$.
(3) Finally, in the regime $a_1 \gtrsim a_0$, all the expansions break down and the structure of the Wigner function has to be analyzed differently.

We concentrate first on the pure adiabatic regime where we have $a_1 \ll a_0$ and $f \ll a_0$. In this regime, the intuition of a thermal response following the evolution of the acceleration works. Furthermore, the overall order of magnitude of a correction to $W[a_\tau]$ coming from the functional and derivative expansions is given by powers of the form $(2\pi f/a_0)^p \cdot (a_1/a_0)^q$. Table II sums this up from the first few corrections.

Thanks to the symmetry of the Wigner function, the first correction in Eq. (29) only has even derivatives in a in the derivative expansion. This means in particular that there is

TABLE II. Orders of magnitude (in units of a_0) of the corrections in the functional and derivative expansion.

$O(\delta a)$		$O(\delta a^2)$		$O(\delta a^3)$	
$(2\pi f)^2 a_1$	$[\ddot{a}]$	$(2\pi f)^2 a_1^2$	$[\dot{a}^2]$	$\varnothing$	
$\varnothing$		$(2\pi f)^3 a_1^2$	$[\dot{a}\,\ddot{a}]$	$(2\pi f)^3 a_1^3$	$[\dot{a}^3]$
$(2\pi f)^4 a_1$	$[a^{(4)}]$	$(2\pi f)^4 a_1^2$	$[\ddot{a}^2]$	$(2\pi f)^4 a_1^3$	$[\dot{a}^2\ddot{a}]$

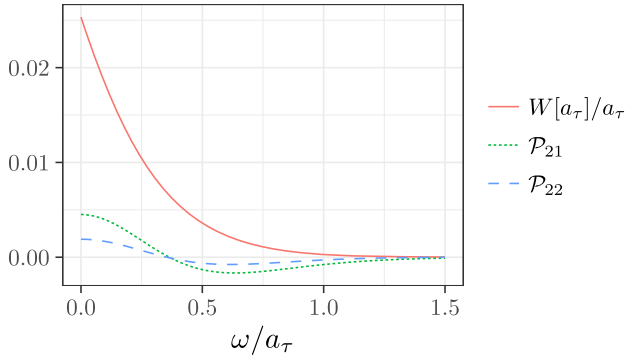

FIG. 2. Representation of the universal functions of the thermal distribution coming as corrections to the pure thermal response $W[a_\tau]$ in the derivative expansion. Their form is independent of the trajectory.

no $\dot{a}$ correction to the thermal behavior. The first two corrections to the Wigner function have the following form:

$$W[a(\tau)] = W[a_\tau] + \frac{\ddot{a}}{a^2}\mathcal{P}_{12}[g](2\pi\omega/a_\tau) + \frac{\dot{a}^2}{a^3}\mathcal{P}_{22}[g](2\pi\omega/a_\tau), \tag{31}$$

where $g(x) = x/(e^x - 1)$ is the thermal distribution, and $\mathcal{P}_{ij} \in \mathbb{R}[Y, X]$ are polynomials of two variables such that the action on f is a derivative operation $\mathcal{P}_{ij}[g] \equiv \mathcal{P}_{ij}(x, \partial_x)[g(x)]$. Technical details about this derivation are given in Appendix B of the Supplemental Material [30]. Figure 2 represents the two functions $\mathcal{P}_{12}[g](x)$ and $\mathcal{P}_{22}[g](x)$, which are universal in the sense that they do not depend on the trajectory of the detector, while Fig. 3 compares each correction to the exact expression evaluated numerically at a given order. This shows that the corrections to the adiabatic thermal response are orders of magnitude less than $W[a_\tau]$, thus justifying that the regime $a_1 \ll a_0$ and $f \ll a_0$ corresponds indeed to an adiabatic regime where the thermal response follows the evolution of the acceleration.

2. Breakdown of the adiabatic regime

When the perturbation is too important, meaning that the conditions $a_1 \ll a_0$ and $f \ll a_0$ are not both fulfilled, the adiabatic response is not valid anymore. The simplest deviation we can first consider is $f \gtrsim a_0$. Intuitively, we expect that, since the frequency is too high, the thermal response cannot build up fast enough and follow the variations of the acceleration. Only an average thermal response at the acceleration $\bar{a}$ should build up, while traces of the oscillations should appear at higher frequencies in the time-frequency plane. This intuition can be explicitly checked by computing exactly the full first correction in Eq. (29) for the trajectory $a(\tau) = a_0 + a_1 \sin(2\pi f \tau)$ denoted $\Delta_0 W$. It actually contains all the derivative

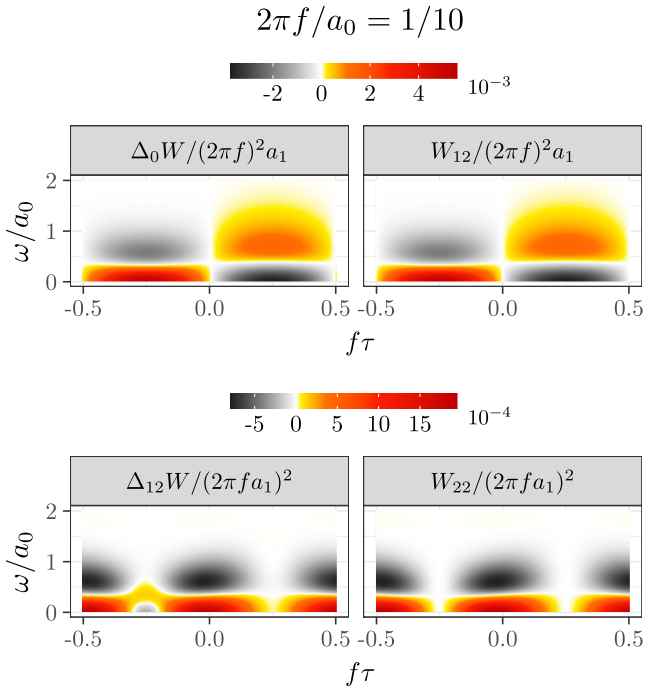

FIG. 3. Comparison between a correction to $W[a_\tau]$ at a given order W_{ij} and the exact one at the same order $\Delta_{ij}W = W - \sum_{(k,l)<(i,j)} W_{kl}$. In the adiabatic regime, at low frequency f, the derivative expansion is meaningful, each correction being an order of magnitude lower than the previous one.

corrections $a^{(n)}$ of order n (first column of Table II). Its explicit form is given by

$$W_1 = \frac{a_1 \sin(2\pi f\tau)}{4\pi^2}\left[\frac{1}{1+(2\pi f/a_\tau)^2}\frac{g_+ + g_-}{2} - \frac{\omega/2\pi f}{1+(2\pi f/a_\tau)^2}(g_+ - g_-) + \frac{2\pi}{a_\tau}\omega\dot{g}_0 - g_0\right], \quad (32)$$

where we reuse $g(x)$, the thermal distribution, and its values $g_\pm = g(2\pi/a(\omega \pm \pi f))$ and $g_0 = g(2\pi\omega/a)$. It can be explicitly checked that in the limit $f \ll a_0$, we recover the $\ddot{a}$ correction to the adiabatic behavior.

From Eq. (32), we can now understand the high-frequency regime $f \gg a$. In the region $\omega \lesssim a_0$, we have

$$W_1 \approx \frac{a_1 \sin(2\pi f\tau)}{4\pi^2}\left[\frac{2\pi}{a_\tau}\omega\dot{g}_0 - g_0\right]. \quad (33)$$

This expression has a nice interpretation: by considering a uniformly accelerated trajectory a_0 perturbed by a constant small term a_1, we have $W[a_0 + a_1] = W[a_0] - [\frac{2\pi}{a_\tau}\omega\dot{g}_0 - g_0]/4\pi^2$. Thus, we conclude that in the region $\omega \lesssim a_0$ in the high-frequency regime, the full Wigner function has the simple expression

$$W[a(\tau)] = W[\bar{a}]. \quad (34)$$

This matches the intuitive idea that the frequency of the perturbation is too high for a thermal behavior following the drive to build up. In fact, by a proper expansion of Eq. (32) in $2\pi f$ (done in Appendix B of the Supplemental Material [30]), we can see that there are corrections of order $1/2\pi f$ to the average thermal response in the frequency band $\omega \in [0, \pi f[$.

Finally, the expansion (29) breaks down completely when the criterion (30) is not satisfied. In the oscillatory example $a(\tau) = a_0 + a_1 \sin(2\pi f\tau)$, this qualitatively means that $a_1 \sim a_0$. In fact, this characterization is too brutal and global compared to the more local one from Eq. (30): this means that globally, the functional expansion cannot be performed, but it can remain meaningful in some time intervals.

Figure 4 represents the Wigner function of the oscillatory acceleration for different parameters $(a_0/2\pi f, a_1/2\pi f)$. The global or local validity of the adiabatic expansion is witnessed by the appearance of inner oscillations in the Wigner function. In the regimes $(4, 1/4)$ and (4,1), for instance, the adiabatic expansion is globally valid. This is no longer the case for the other regimes, where $a_1 \sim a_0$ and where the signal basically goes (close) to zero at some moments in time. Still, the expansion remains locally meaningful half a period later. This can be made more quantitative by explicitly analyzing the criterion (30). As an example, consider the situation where $a_1 = a_0$. The criterion is then equivalent to $\cos(2\pi f\tau + \pi f\upsilon)\sin(\pi f\upsilon) \ll \cos^2(\pi/4 - \pi f t)$. Clearly, when $f\tau = -1/4$, the criterion cannot be satisfied and the adiabatic expansion breaks down, while it is valid around $f\tau = 1/4$ (see Fig. 4). How this can be interpreted will be discussed in more detail in Sec. V.

3. A more physical trajectory

The previous analyses, while important in their own regard to understanding how the response changes in nonstationary situations, are still based on nonphysical trajectories, since they require an infinite amount of energy to be sustained. The question then remains one of understanding the form of the Wigner function for physical trajectories [25,31,32].

Figure 5 represents the Wigner function (left panel) of a trajectory uniformly accelerated for a finite duration $a\tau = 4$. To make contact with the literature, it also shows the Page distribution for the same trajectory (right panel). We can see that a thermal response is building up over a timescale of a few a. It is to be noted that the Page distribution, like the Wigner function, is not always positive in the time-frequency plane.

Concerning the Wigner function, its general features can be well understood. First, we see that a thermal response at temperature $a/2\pi$ appears over a timescale of the order of a. Second, the high-frequency structure around the beginning of the accelerated phase depends solely on the

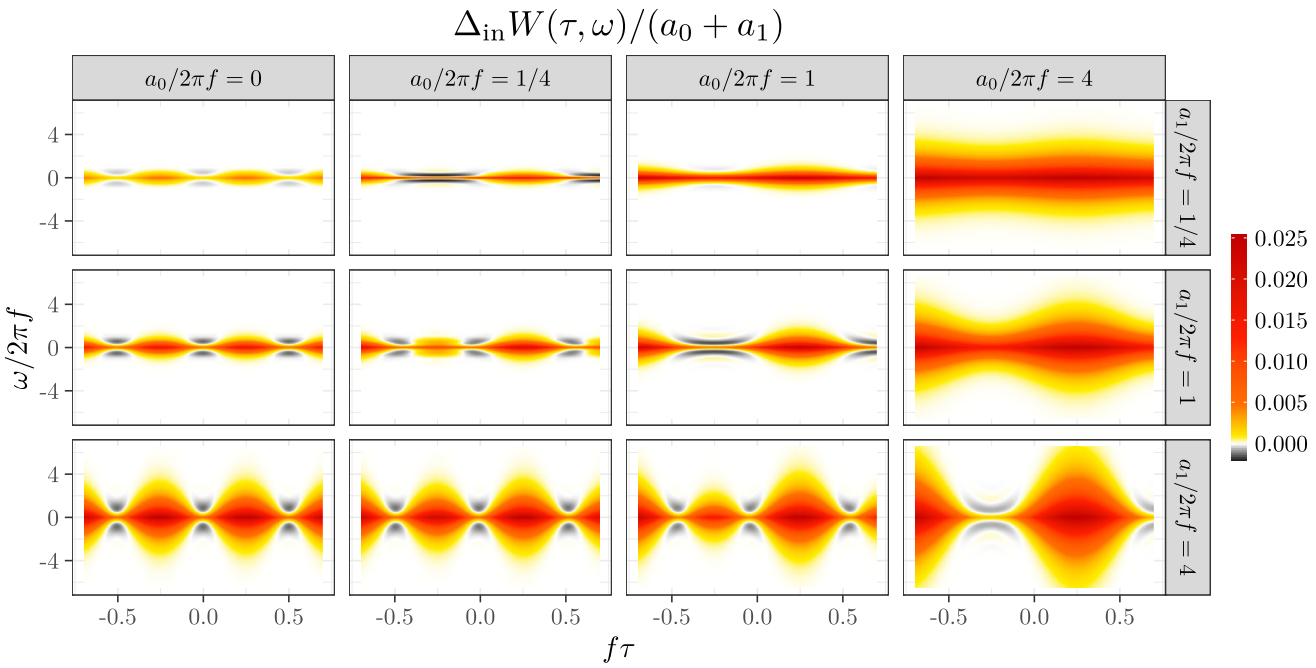

FIG. 4. Wigner function representation of an oscillatory acceleration $a(\tau)=a_0+a_1\sin(2\pi f\tau)$ in different regimes controlled by the expansion parameters $(a_0/2\pi f)$ and (a_1/a_0). In the regime of small frequency f and amplitude a_1 compared to a_0, the adiabatic response works globally. Outside this regime, the adiabatic expansion breaks down, which is witnessed by the appearance of inner oscillations, but can still be meaningful locally.

discontinuity in the acceleration. In our case of interest, we expect the second and higher derivatives of the first-order correlation to be discontinuous. To analyze their effects on the Wigner representation, it is useful to use the following decomposition: $G(\tau+\upsilon/2,\tau-\upsilon/2)=f_\tau(\upsilon)+g_\tau(\upsilon)$, where f contains the lower-order discontinuity contribution and g the higher-order ones. The detailed forms of these functions are irrelevant for the high-frequency behavior and can be chosen for computational convenience: the only constraints are that they should capture the form of the discontinuities

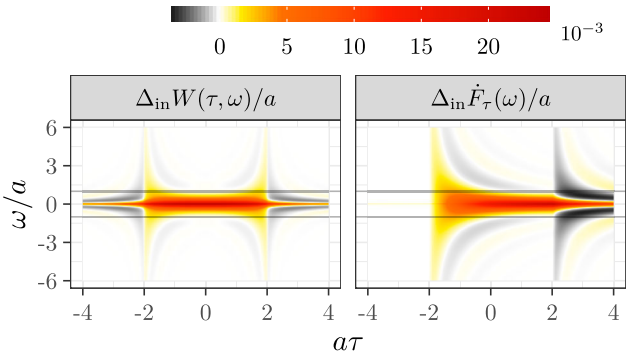

FIG. 5. Wigner (left) and Page (right) distributions of the vacuum for a finite-duration uniform acceleration between two inertial phases. After a transition time of the order of a^{-1}, the thermal behavior at temperature $a/2\pi$ settles down. The decreasing oscillating high-frequency parts are solely controlled by the discontinuity of the acceleration.

(see Appendix A of the Supplemental Material [30] for details on this strategy). In the end, we obtain the high-frequency behavior of the Wigner function around the times τ_d of brutal discontinuous changes of the acceleration:

$$\Delta W(\tau\geq\tau_d,\omega)\simeq-\frac{1}{4\pi^2}\frac{a}{8\sinh^2 a(\tau-\tau_d)}\frac{\sin 2\omega(\tau-\tau_d)}{(\omega/a)^3}, \tag{35a}$$

$$\Delta W(\tau\leq\tau_d,\omega)\simeq-\frac{1}{4\pi^2}\frac{a}{16a^3(\tau-\tau_d)^3}\frac{\cos 2\omega(\tau-\tau_d)}{(\omega/a)^4}. \tag{35b}$$

IV. EXCESS CORRELATION FOR DIFFERENT TRAJECTORIES

Up to now, we have only been interested in the first-order correlation of the vacuum. We now move to the subject of the excitations above the vacuum and how they are perceived by a moving detector [33]. From Eq. (8), the excess correlation coming from a one-particle excitation in a wave function $\Phi(t,\mathbf{x})$ is given by

$$\Delta G_\rho(\tau_2,\tau_1)=\Phi^*(\tau_1)\Phi(\tau_2)+\Phi(\tau_1)\Phi(\tau_2)+\text{H.c.} \tag{36}$$

The nice feature of this correlation function is that its form is independent of the trajectory of the detector, which is a

direct consequence of the covariance properties of the quantum field correlation functions.

The states mostly considered in a quantum optics setting are Fock states and coherent states. The main difference between the two in the first-order correlation is the absence (presence) of the interference terms $\Phi(\tau_1)\Phi(\tau_2) + \text{H.c.}$ for Fock states (coherent states).

Finally, those states can be prepared in different wave packets like a monochromatic one or a Gaussian one. In what follows, we will mainly focus on Gaussian wave packets of coherent and Fock states, which are, in the end, the most intuitive ones. We leave the mathematical analysis of the monochromatic case for Appendix C of the Supplemental Material [30].

A. Gaussian wave packet

Let us consider, for now in $(3+1)$D, that the inertial observer prepares the field in a Gaussian coherent state. It is defined in the following way:

$$|\alpha\rangle = \bigotimes_{\mathbf{p}} |\alpha_{\mathbf{p}}\rangle = e^{\int_{\mathbb{R}^3} (\alpha_{\mathbf{p}} a_{\mathbf{p}}^\dagger - \alpha_{\mathbf{p}}^* a_{\mathbf{p}}) \mathrm{d}^3 p} |0\rangle. \tag{37}$$

The exponential operator is called the displacement operator $D(\alpha)$. This state is normalized and satisfies the fundamental relations of coherent states[1]:

$$D(-\alpha) a_{\mathbf{p}} D(\alpha) = a_{\mathbf{p}} + (2\pi)^3 2\omega_{\mathbf{p}} \alpha_{\mathbf{p}}, \tag{38a}$$

$$a_{\mathbf{p}} |\alpha\rangle = (2\pi)^3 2\omega_{\mathbf{p}} \alpha_{\mathbf{p}} |\alpha\rangle. \tag{38b}$$

We can also think of this state in a spatial way by looking at its action on a field operator. Indeed,

$$D(-\alpha)\phi^+(x,t)D(\alpha) = \phi^+(x,t) + \Phi_\alpha(x,t), \tag{39}$$

where ϕ^+ is the negative-frequency part of the field. Thus, we see that the state (37) is a coherent state in position with a parameter given by

$$\Phi_\alpha(x,t) = \int_{\mathbb{R}^3} \alpha_{\mathbf{p}} e^{-i(w_{\mathbf{p}} t - \mathbf{p}.\mathbf{x})} \mathrm{d}^3 p. \tag{40}$$

We see that at $t = 0$, this is just the Fourier transform of the coherent-state parameter in momentum space. From the factorized nature of this state, the first-order correlation function can be decomposed into clear different contributions:

$$\Delta G_{|\alpha\rangle}(\tau_2,\tau_1) = \Phi_\alpha(\tau_1)\Phi_\alpha(\tau_2) + \Phi_\alpha(\tau_1)\Phi_\alpha^*(\tau_2) + \text{H.c.} \tag{41}$$

[1]This is obtained from the BCH formula and the covariant commutation relations $[a_{\mathbf{p}}, a_{\mathbf{p}'}^\dagger] = (2\pi)^3 2\omega_{\mathbf{p}} \delta(\mathbf{p} - \mathbf{p}')$.

We now specify the function $\alpha_{\mathbf{p}}$ and choose it so that the problem reduces effectively to a $(1+1)$D problem for computational simplicity. We then consider a Gaussian centered at a given momentum p_0, with a width given by σ_p. We then have

$$\alpha_p = \sqrt{\frac{p_0}{2\pi}} \frac{1}{(2\pi\sigma_p^2)^{1/4}} e^{-\frac{(p-p_0)^2}{4\sigma_p^2}} e^{-ip.x_0}. \tag{42}$$

In position, it is a Gaussian centered at the position x_0. We also make the assumption that $p_0 \gg \sigma_p$ so that we can consider $\omega_p = |p| = p$ in our computations. This leads to

$$\Phi_\alpha(\tau) = \sqrt{\frac{p_0}{(2\pi\sigma_x^2)^{1/2}}} e^{-[(t_\tau - x_\tau) + x_0]^2/4\sigma_x^2} e^{-ip_0[(t_\tau - x_\tau) + x_0]}. \tag{43}$$

The introduction of the normalization $\sqrt{p_0/2\pi}$ comes from dimensional considerations, since we require the average energy to equal the average value of the Wigner function over time and frequency [see Eq. (21)]. We also introduce the position width σ_x satisfying the relation $\sigma_x \sigma_p = 1/2$.

As an example, consider an inertial trajectory with a velocity v; the worldline is parametrized as $(\gamma\tau, \gamma v\tau)$. Its Wigner function is

$$W^{(v)}(\tau,\omega) = 2p_0 \left[e^{-\frac{(\omega - D_v p_0)^2}{2(D_v\sigma_p)^2}} + e^{-\frac{(\omega + D_v p_0)^2}{2(D_v\sigma_p)^2}} + 2\cos\left(2p_0(D_v\tau + x_0)\right) e^{-\frac{\omega^2}{2(D_v\sigma_p)^2}} \right] e^{-\frac{(D_v\tau + x_0)^2}{2\sigma_x^2}}. \tag{44}$$

The computation is straightforward, and the Wigner function is composed of two symmetric Gaussian spots centered around the Doppler-shifted frequency $D_v p_0$ with their interference pattern.

Gaussian spots are in fact the basic "atoms" of the Wigner function and allow us to understand the geometry behind this representation [16]. The basic interpretative element that we need and that we see in Eq. (44) is that the interference term of two Gaussian atoms is also a Gaussian spot located at the midpoint joining the center of the two atoms (here $\omega = 0$) and that the interference pattern oscillates in the orthogonal direction.

This discussion would be completely similar if, instead of Gaussian coherent states, we considered a Gaussian superposition of a Fock state of n photons. The excess correlation is even simpler, since the interference terms vanish: $\Delta G_{|n_\alpha\rangle} = n\Phi_{n_\alpha}^* \Phi_{n_\alpha} + \text{H.c.}$

While those Wigner functions could have been guessed intuitively for an inertial response, it is a nontrivial task to analyze the response to a Gaussian excitation from a moving detector for different accelerated trajectories.

B. Accelerated Wigner function

1. Uniformly accelerated case

Suppose now that the Gaussian coherent state, prepared by the inertial observer, is probed by a uniformly accelerated detector following the worldline $(a^{-1}\sinh a\tau, a^{-1}(\cosh a\tau - 1))$ in $(1+1)$D. Figure 6 shows the Wigner functions of both Fock and coherent Gaussian states evaluated numerically. Each snapshot represents the Wigner function for a pulse emitted at a different position x_0. As intuition would suggest, the closer the emission is to the horizon, the more redshifted and deformed the wave packet is.

A closed analytical form cannot be obtained in this case, but the structure of the Wigner function can be completely understood using Gaussian and stationary phase approximation schemes and its first correction. A detailed treatment is given in Appendix D of the Supplemental Material [30]. For clarity, let us focus on the $\Phi_\alpha(t,x)\Phi^*_\alpha(t',x')$ contribution of the Wigner obtained from Eq. (43) evaluated on the uniformly accelerated trajectory.

The first approximation scheme that we can employ is to approximate the received wave packet by a Gaussian function around its maximum reached at time τ_r. Physically, this is the time of reception for the moving detector. It is obtained by solving $t_\tau - x_\tau + x_0 = 0$, which gives the special relativistic result

$$\tau_r = -a^{-1}\ln(1+ax_0). \tag{45}$$

Computing the Wigner function is then straightforward and gives

$$W_{\Phi_a\Phi^*_a}(\tau,\omega) = \frac{2p_0}{D_r}\exp\left(-\frac{D_r^2}{2\sigma_x^2}(\tau-\tau_r)^2\right) \exp\left(-\frac{1}{2}\frac{4\sigma_x^2}{D_r^2}(\omega-\omega_r(1-a(\tau-\tau_r)))^2\right), \tag{46}$$

with $D_r = e^{-a\tau_r}$ being the "gravitational" redshift and ω_r the shifted frequency measured by the moving detector,

$$\omega_r = p_0 e^{-a\tau_r} = p_0(1+ax_0). \tag{47}$$

This is the uniformly accelerated analogue of the Einstein effect. Thus, we recover directly at this level of approximation the standard results of light perceived by a uniformly accelerated observer in a special relativistic setting.

While this rough Gaussian approximation allows us to pinpoint the dominant part of the Wigner function in the time-frequency plane, it is not well suited to understanding the inner interference pattern. However, the stationary phase approximation scheme can. Writing the Wigner function as $W_{\Phi_a\Phi^*_a}(\tau,\omega) = \int_{\mathbb{R}} A(v;\tau)e^{i\Phi(v;\tau,\omega)}dv$, the stationary phase is meaningful when the velocity of phase oscillations is larger than the variations of the modulus. This is indeed the case here, since the phase blows up exponentially compared to the Gaussian decay of the

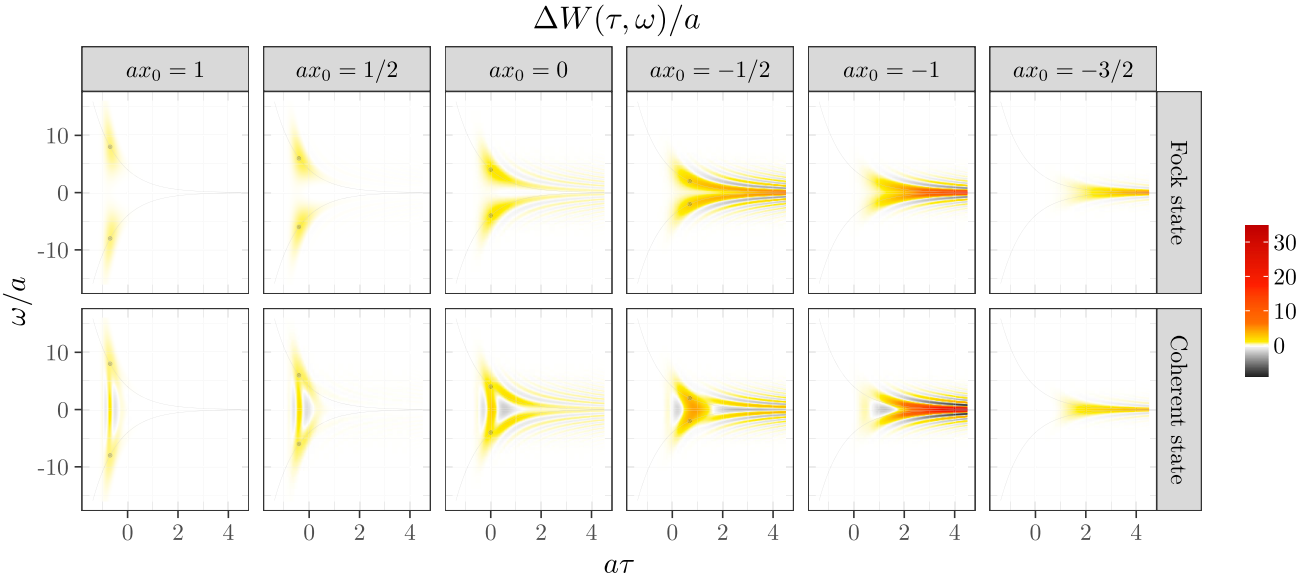

FIG. 6. Evolution of the Wigner function of the Gaussian Fock state (top row) and coherent state (bottom row) emitted at different positions x_0, with a frequency $p_0/a = 4$ and a width $a\sigma_x = 1/2$ in the inertial frame. The signal is centered around a spot at (τ_r,ω_r) given by Eqs. (45) and (47), which are the special relativistic reception time and frequency, respectively, and follow the instantaneous frequency curve for different x_0. As the emission gets closer to the horizon, the spot flattens and gets strongly redshifted.

modulus. Now, we have to find the stationary points and compute the derivatives at those points. The stationary points τ_s are solutions of

$$\frac{\partial\Phi}{\partial v}(\tau_s;\tau,\omega)=0\Rightarrow\begin{cases}\frac{\omega}{p_0}e^{a\tau}=\cosh a\tau_s/2, & \frac{\omega}{p_0}e^{a\tau}\geq 1\\ \varnothing & \text{otherwise}\end{cases}. \tag{48}$$

We have two symmetric solutions, τ_s and $-\tau_s$. The condition of existence shows that the stationary phase approximation is defined in the convex hull of the instantaneous frequency curve $\omega(\tau)=p_0e^{-a\tau}$. The second derivative evaluated at τ_s gives the validity domain of the stationary phase approximation. On the positive solution τ_s,

$$\begin{aligned}\frac{\partial^2\Phi}{\partial v^2}(\tau_s;\tau,\omega)&=-\frac{a}{2}\omega(\tau)\sinh\left(\operatorname{arcosh}\left(\frac{\omega}{\omega(\tau)}\right)\right)\\ &\underset{\tau_s>0}{\Rightarrow}\frac{\partial^2\Phi}{\partial v^2}(\tau_s;\tau,\omega)=-\frac{a}{2}\sqrt{\omega^2-\omega^2(\tau)}\leq 0.\end{aligned} \tag{49}$$

Away from the instantaneous curve and inside its convex hull, the Wigner function is well approximated by the stationary phase approximation. Its explicit derivation is given in Appendix D of the Supplemental Material [30], and we have

$$\begin{aligned}W_{\Phi_a\Phi_a^*}(\tau,\omega)=&\sqrt{\frac{8p_0^2}{a\sigma_x^2}}\frac{\exp\left(-\frac{(\omega-\omega_r)^2+[\omega-\omega(t)][\omega+\omega(t)]}{2(ap_0\sigma_x)^2}\right)}{\sqrt{\omega^2-\omega^2(t)}}\\ &\times\cos\left(2\left[\frac{1-\ln 2}{a}-\tau\right]\omega+\frac{\pi}{4}\right).\end{aligned} \tag{50}$$

This form can be interpreted as follows: First, oscillations are present in the Wigner function, given by the cosine term, covering the whole time-frequency plane. Second, the dominant contribution is at the intersection of a strip centered around the frequency ω_r and a tube following the instantaneous frequency $\omega(t)$. This allows us to understand pictorially why interferences appear as we get closer to the horizon: the intersection region gets wider as we get closer, allowing the interferences to be visible.

To be rigorous, the approximation fails on the instantaneous curve $\omega(\tau)$. We should then go to the next order of approximation: this is the Airy approximation. Fortunately, since $\frac{\partial^3\Phi}{\partial\tau^3}(\tau_s;\tau,\omega(\tau))\neq 0$, we do not need to go to a higher order. The behavior of the Airy function is controlled by the curvature $\epsilon(\tau)$ of the instantaneous frequency:

$$\epsilon(\tau)=\frac{1}{4\pi}\left(\frac{\mathrm{d}^2\omega(\tau)}{\mathrm{d}t^2}\right)^{1/3}=\frac{(a^2\omega(\tau))^{1/3}}{4\pi}. \tag{51}$$

Nonetheless, the stationary phase approximation (and its corrections) of the Wigner function gives already the general qualitative structure of the oscillations that we can see in Fig. 6.

2. *General* $(1+1)$D *trajectory*

For a generic trajectory, it is, of course, not possible to obtain a complete analytical form of the Wigner function. Nonetheless, its general features are clearly obtained from the Gaussian and stationary phase approximations that we already used for the uniformly accelerated case. Indeed, from the detailed computations presented in Appendix D of the Supplemental Material [30], we can prove the intuitive idea that first the Gaussian spot is shifted in the time-frequency plane by the "gravitational" redshift. The instantaneous frequency curve that the spot is following is given by (see Sec. III A for the notations)

$$\omega(\tau)=p_0e^{-A(\tau)}\quad\text{with}\quad A(\tau)=\int_0^\tau a(u)\mathrm{d}u. \tag{52}$$

The spot is centered around the reception time τ_r which is a solution of the equation $\int_0^{\tau_r}\exp(-A(u))\mathrm{d}u=-x_0$. Since the term in the integrand is positive, this equation possesses either no solution or a single solution. This comes from the fact that the observer necessarily travels slower than the speed of light. As such, it is only possible to meet the photon once. If this equation has no solution, it means that the photon was emitted behind the event horizon of the observer. We note that, at this order of approximation, the chirp rate is what we classically expect: it is given by the variation of the frequency shift for different times, which is here $\frac{\mathrm{d}\omega(\tau)}{\mathrm{d}\tau}=-a(\tau)\omega(\tau)$.

The inner interference pattern (inside the convex hull defined by the instantaneous frequency curve) is once again understood by resorting to the stationary phase approximation and its Airy correction.

Figure 7 shows the response of a moving detector following a trajectory uniformly accelerated by parts. Starting from inertial motion, the first phase of the motion accelerates uniformly with acceleration a at time $a\tau=-2$ until time $a\tau=-1$. The second phase, between $a\tau=-1$ and $a\tau=1$, has acceleration $-a$. The last phase again has acceleration a until $a\tau=2$ with inertial motion onward. This is the kind of trajectory considered in the twin paradox setup. The signal follows the instantaneous frequency curve, which can be computed exactly in this case, and the wave packet is deformed, chirped, along it.

C. Transformation of coherence

The mathematical framework developed so far is also well suited to analyze superpositions. Let us again consider a one-particle excitation which is now prepared in a wave

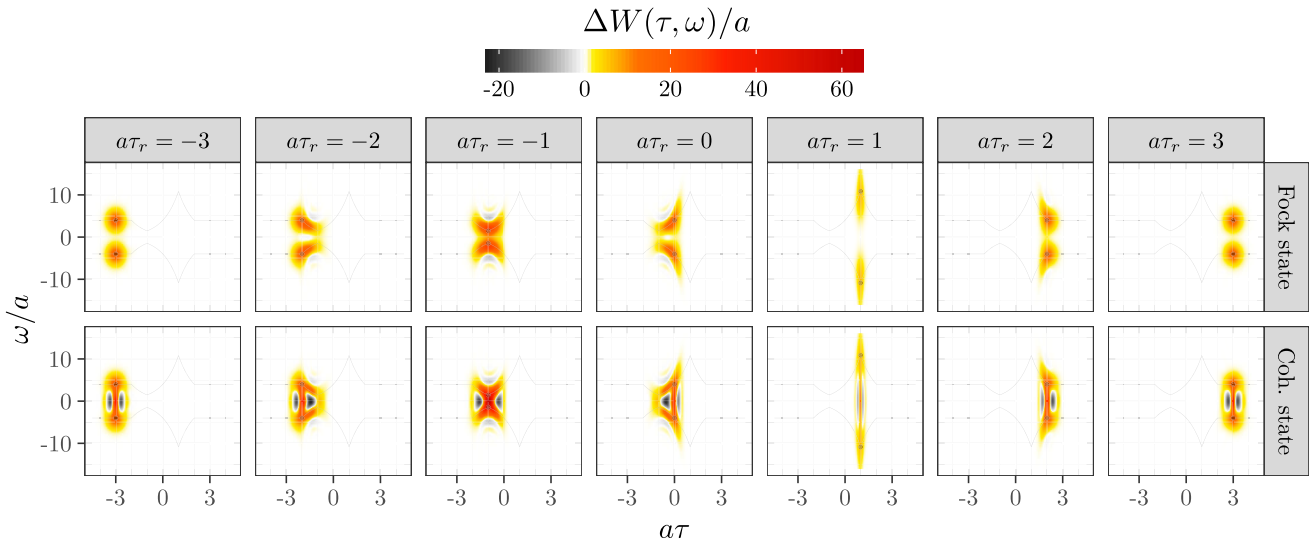

FIG. 7. Wigner function representations of a Gaussian Fock state (top row) and Gaussian coherent state (bottom row) probed by a detector following a uniformly accelerated twinlike trajectory: the spot is chirped by the accelerated motion with a rate $-a(\tau)\omega(\tau)$ but follows the instantaneous frequency curve. The total time of the accelerating phase is $a\tau_{\rm acc} = 4$, with transitions at $\tau = -2, -1, 1, 2$. The frequency of the wave packet in the inertial frame is $p_0/a = 4$, and its width is $a\sigma_x = 1/3$.

packet $\Phi(x)$ composed of a linear combination of elementary ones $\Phi_k(x)$ as

$$\Phi(x) = \sum_k a_k \Phi_k(x). \tag{53}$$

In this case, it is straightforward to show that

$$\Delta W(\tau,\omega) = \sum_{k,k'} a^*_{k'} a_k \Delta W_{kk'}(\tau,\omega), \tag{54}$$

where we have introduced the notation

$$\Delta W_{kk'}(\tau,\omega) = \int_{\mathbb{R}} \Phi^*_{k'}(\tau - \upsilon/2)\Phi_k(\tau + \upsilon/2)e^{i\omega\upsilon}\mathrm{d}\upsilon. \tag{55}$$

When $k = k'$, we recognize that $\Delta W_{kk'}$ is the excess Wigner function in the presence of the excitation Φ_k. Furthermore, $k \neq k'$ indicates cross terms, responsible for the so-called outer interference terms, between the different components Φ_k. These interferences were already present in Figs. 6 and 7 for the Gaussian coherent state. The total excess Wigner function can thus be expressed as a sum containing the main components and cross terms:

$$\Delta W(\tau,\omega) = \sum_k |a_k|^2 \Delta W_{kk}(\tau,\omega) + \sum_{k\neq k'} a^*_{k'} a_k \Delta W_{kk'}(\tau,\omega). \tag{56}$$

The important message here is that the excess terms deform naturally. If we start with some spatial superposition, each term will be deformed as if it were alone. At the same time, the outer interference terms depend only on the deformed wave packets. This means that if we emit a wave packet in a linear superposition of two wave packets received around times τ_1 and τ_2, we expect that the interference terms will be located at the midpoint $\tau_m = (\tau_1 + \tau_2)/2$. Furthermore, those interference terms will not depend on the details of the trajectory at time τ_m, but on those at the times of reception τ_1 and τ_2.

Figure 8 considers once again the uniformly accelerated twinlike trajectory of Sec. IV B 2. The field is, however, prepared in a spatial superposition of two Gaussian wave packets (only the photon wave function is represented for clarity):

$$\Phi(x) = \Phi_2(x) + \Phi_1(x), \tag{57}$$

where the wave packet $\Phi_i(x)$ is centered around the position x_i and is received by an inertial observer at time t_{r_i} and by the moving detector at times τ_{r_i}. Quite naturally, the structure of the Wigner function depends on the spatial separation of the components of the superposition, or equivalently, on the detection times and the local characteristics of the trajectory.

First, by denoting $\mathcal{J}^-(x)$ the causal past of a point x in spacetime, the coherence properties are modified by the motion of the detector only if at least one component has been prepared in the spacetime region $\mathcal{J}^-(f)\backslash\mathcal{J}^-(i)$, where i and f are the beginning and end events of the acceleration phase, respectively.

The second feature concerns the delay time between the reception of the two wave packets. In Fig. 8, the wave packets were prepared such that the inertial delay $\Delta t_r = 4a^{-1}\sinh(a\Delta\tau_r/4)$ with $\Delta\tau_r = 3$, which is the

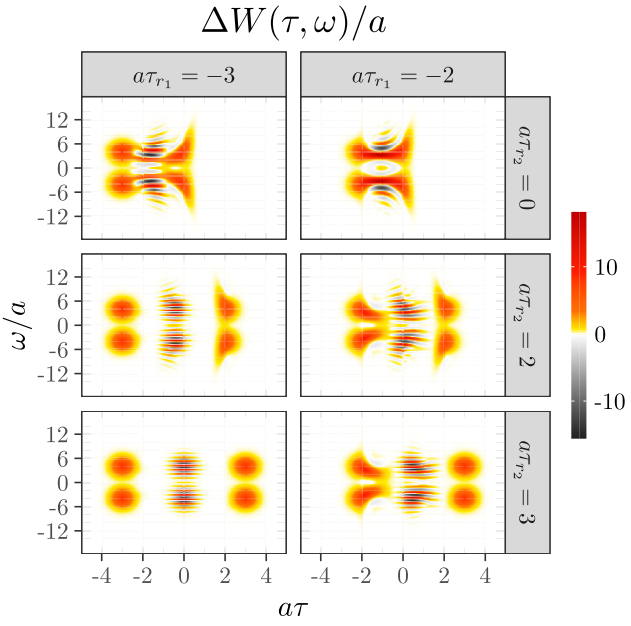

FIG. 8. Wigner function representation of a superposition of a Gaussian photon wave packet probed by a detector following a uniformly accelerated twinlike trajectory for different $\tau_{r,1}$ and $\tau_{r,2}$ reception times associated with the first and second components of the superposition, respectively. The total time of the accelerating phase is $a\tau_{\mathrm{acc}} = 4$ with transitions at $\tau = -2, -1, 1, 2$. The wave packet is emitted at frequency $p_0/a = 4$ in the inertial frame with a width $a\sigma_x = 1/3$.

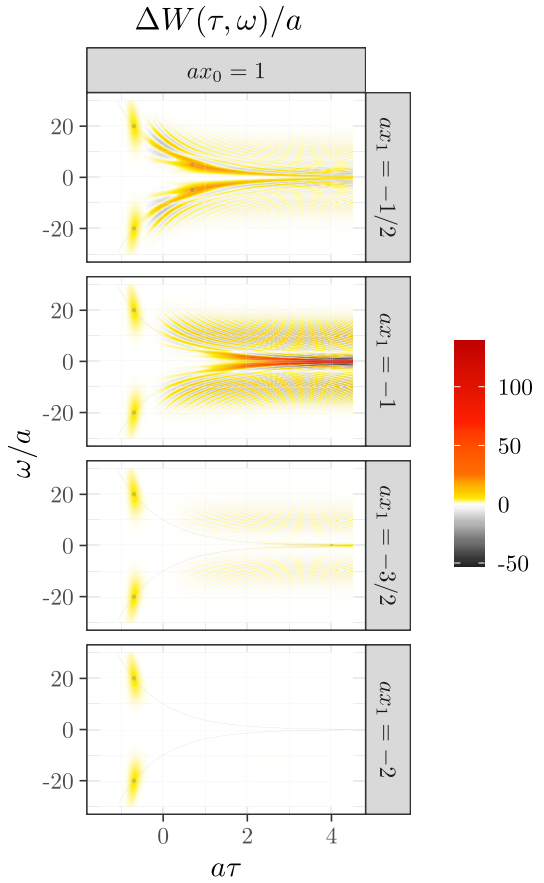

FIG. 9. Wigner function representations of a Gaussian superposition received at different times for a uniformly accelerated observer. The coherences are spread and eventually lost when a member of the superposition gets close to or crosses the horizon. The wave packet is emitted at frequency $p_0/a = 10$ in the inertial frame with a width $a\sigma_x = 1/5$.

general twin paradox delay formula for this trajectory. This time delay is clearly seen in the Wigner function and satisfies the special relativistic result (Fig. 2 of the Supplemental Material [30] compares the inertial and accelerated responses directly).

Finally, while the coherence pattern is identical to a pure inertial response when the packets are prepared outside the region $\mathcal{J}^-(f)\backslash\mathcal{J}^-(i)$, the interference pattern is clearly deformed by the motion of the detector when one component is probed in the accelerated phase.

Figure 9 shows the more extreme case of the evolution of coherence of a Gaussian superposition probed by a uniformly accelerated detector. The spacetime geometry probed by this detector, also called Rindler spacetime or wedge, is quite different from the previous case because of the presence of an event horizon. Naturally, a detection event occurs if and only if the wave function has been prepared with a support in the wedge. The situation shown in Fig. 9 represents a Gaussian superposition of two wave packets, one of which propagates closer and closer to the horizon. The coherence gets spread and redshifted as the wave packet approaches the horizon, which is a consequence of the same effects happening to the wave packet itself.

After crossing the horizon, no detection signals can be recovered by the detector, and the coherences are lost. This is, of course, the same effect happening in black hole physics which leads to the famous information paradox. We should note that this loss of coherence cannot be properly qualified as a decoherence process in the traditional sense, where an environment interacts with the system and attenuates the interference pattern. Indeed, the deformation and loss of coherence only comes about because the wave packets themselves are deformed by motion or lost behind a horizon, which is not what decoherence is about.

V. DISCUSSIONS

So far, the point of view we adopted was a pure signal processing one. Indeed, our interest was only focused on doing a proper analysis of signals characterized by correlation functions $G_\rho(\tau_1, \ldots, \tau_n)$ obtained from a set of pointlike detectors. The question remains of how to relate those signals to quantum field theories for different observers [6,34,35].

The fundamental question at this stage is to understand what can be reconstructed about the quantum field from the

signals (of one or a set of detectors). To be more precise, we can roughly group the questions in two categories:

(1) What can we learn about the trajectory of the detector with respect to the laboratory frame θ?
(2) Can we reconstruct a field-theoretic picture $(\mathcal{H}_\theta, f_\theta)$ from the signals, with $\mathcal{H}_\theta$ being the Hilbert space of the theory and f_θ the mode on which the field is decomposed?

Our signal processing approach opens up some interesting perspectives on these questions.

Concerning the recovery of information about the trajectory, we need prior information about what was sent by the laboratory. Indeed, it is conceivable to imagine only inertial detectors probing a state prepared in such a way as to simulate an accelerated response. So, in order not to be fooled by what we measure, we need, for instance, the laboratory to communicate to the accelerated observer what they originally prepared. Information about the trajectory can then be recovered by properly fitting the measured signal or, if we have enough data, reconstructing the instantaneous frequency curve from which the acceleration can be deduced since $\mathrm{d}\omega(\tau)/\mathrm{d}\tau = -a(\tau)\omega(\tau)$. If no excitations are present, we can still have some information about the trajectory from the power spectrum [Eq. (28)] of the vacuum: indeed, for a one-dimensional motion, it is directly proportional to the square of the acceleration.

The second question was about reconstructing a field-theoretic or many-body point of view from the signals. While we are not going to investigate this complicated question thoroughly, time-frequency analysis can shed some light on one particular issue concerning the definition of a notion of particles.

In the standard many-body approach, there is no issue with defining a notion of particles in a stationary situation [36] like a uniformly accelerated motion. Qualitatively, we have a notion of time from which we can define a Fourier transform. There is, however, no general method to defining a notion of particles in nonstationary situations. In other words, the notion of particles is an emerging notion [37]. It is nonetheless interesting to link this emerging notion to the notion encountered in the standard many-body approach.

One way to do this is to introduce an operational notion of particles thanks to response signals $G(\tau_1, \tau_2)$ of detectors [4]. The question is to then relate those two notions which, in general, are quite different. As we already mentioned, it is valid to interpret $G_\rho(\omega, \omega')$ in terms of excitations for inertial detectors as is usually done, for instance, in quantum optics: the two notions coincide. This breaks down *a priori* in nonstationary motions.

The time-frequency analysis of the complete signal offers a strategy to link the two notions and reconstruct a many-body particle interpretation. Indeed, from the full signal, it is possible to extract stationary domains [38]. Intuitively speaking, we can extract domains where it is meaningful to decompose the field modes like $f_{\mathbf{p}}(\tau, \mathbf{r}) \propto e^{-i\omega_{\mathbf{p}}\tau} f_{\mathbf{p}}(\mathbf{r})$ [6]. Knowing then the stationary time scales and averaging the signal over them, notions of particles could then be locally defined. Operationally speaking, what can be done is to consider a detector with a response function having support on those domains.

To illustrate this strategy, let us consider again the situation studied in Sec. III B, where we considered an oscillatory motion of the form $a(\tau) = a_0 + a_1 \sin(2\pi f\tau)$ represented in Fig. 4. This situation is completely nonstationary and even not globally adiabatic when $a_0 = a_1$. No natural particle interpretation can be found. Nonetheless, we know that we can consider the signal as approximately stationary around a given time τ over a timescale τ_s (depending itself on τ): this is the same condition controlling the validity of the functional expansion Eq. (29).

In a given signal, different stationary timescales exist, as we discussed already in Sec. III B 2. Figure 10 represents the (Gaussian) average of the Wigner function around a time τ with a time window of typical width τ_s: only a section is represented (it is sufficient, since we are approximately stationary) and corresponds to the averaged energy distribution $f_w(\omega)$. To be consistent and respect the Heisenberg time-frequency indeterminacy, a (Gaussian) average should be performed in frequency: this frequency window is the orange area in Fig. 10 where two extreme cases are shown:

(1) At the maximum of acceleration (where the adiabatic regime is valid, $f\tau = 1/4$), the distribution $f_w(\omega)$ is a thermal distribution at a temperature around a_τ. The frequency average is such that the overall time-frequency response of a detector with a response function of width τ_s around $f\tau = 1/4$ will be a stationary thermal distribution. We can then reconstruct in this time-frequency domain a uniformly accelerated particle picture.
(2) At lower accelerations, the distribution $f_w(\omega)$ looks thermal but has to be averaged over a very large

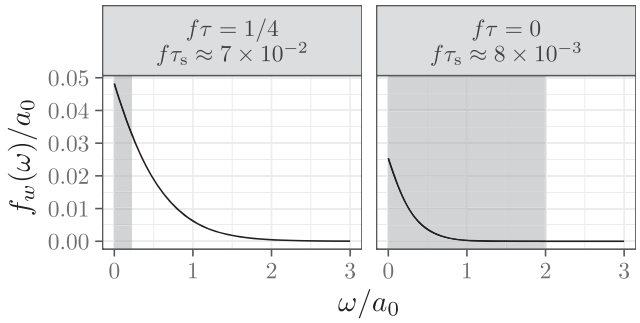

FIG. 10. Gaussian average of the Wigner function over a window given by τ_s such that $|a/\delta a| \leq 1/20$ for the sine case, where $a_0 = a_1$, and $2\pi f/a_0 = 1/5$. To have a consistent time-frequency representation, we need to perform another Gaussian average of typical spread, given by the shaded area which depends on τ_s. A particle picture is meaningful only above this frequency threshold.

frequency domain compared to its typical width. This is a consequence of the very low stationary timescale there. In this case, the only meaningful particle picture that can be constructed is at very high frequencies and matches that of an inertial response. This follows the intuition that high-frequency modes are equal to inertial modes.

In the end, the main lesson from this discussion is that particles emerge from the signal, and applying a time-frequency analysis seems the most appropriate way to tackle the issue of particle reconstruction and to link the operational and many-body definitions.

VI. CONCLUSION

In this paper, we introduced a signal processing time-frequency approach to the problem of detectors in motion in relativistic quantum field theory. It offers a natural and synthetic framework to analyze nonstationary trajectories. We provided a detailed analysis of the adiabatic regime, its corrections, and its breakdown. We then moved on to study how excitations are probed by a moving detector, focusing for clarity on Gaussian states. The structure of the Wigner function can be completely understood using simple approximation schemes. Beside recovering time-frequency special relativistic behaviors in general frames, we were able to analyze how wave packets and their coherence properties are transformed by the motion of the detector.

We finally used our analysis of excitation and motion to discuss how time-frequency analysis provides a promising approach to clarify conceptual questions behind the problem of moving detectors, especially concerning the definitions of a notion of particles. Indeed, time-frequency allows us to define a notion of relative stationary timescales over the signal, permitting us to locally link the operational and many-body definitions of particles.

Apart from those conceptual questions, this time-frequency signal processing approach opens up many interesting perspectives to sharpen our understanding of relativistic detectors. Indeed, a natural generalization is to analyze higher-order correlation functions, which play an important role in quantum optics. This would allow us to understand from first principles the interplay between entanglement [39,40], which is encoded in the second-order correlation function, and motion in a completely relativistic setting. Moreover, one of the main challenges is to have experimental access to the Wigner function. Measuring the Wigner is traditionally done through an interferometric setup like the Hong-Ou-Mandel experiment. This then demands a proper analysis of those interferometric experiments when probed by a moving detector. Finally, the same approach could be generalized to curved spacetime, allowing us again to understand the response of the detector in nonstationary spacetime situations like the formation of black holes by a collapsing star or the effect of gravitation on the entanglement of quantum systems.

ACKNOWLEDGMENTS

We thank P. Degiovanni and G. Fève for useful discussions. We also thank J.-M. Raimond for useful remarks on our manuscript.

[1] S. Hollands and K. Sanders, *Entanglement Measures and Their Properties in Quantum Field Theory* (Springer, New York, 2018), Vol. 34.
[2] E. Witten, Notes on some entanglement properties of quantum field theory, Rev. Mod. Phys. **90**, 045003 (2018).
[3] S. W. Hawking, Particle creation by black holes, Commun. Math. Phys. **43**, 199 (1975).
[4] W. G. Unruh, Notes on black-hole evaporation, Phys. Rev. D **14**, 870 (1976).
[5] S. Schlicht, Considerations on the Unruh effect: Causality and regularization, Classical Quantum Gravity **21**, 4647 (2004).
[6] P. Grove and A. C. Ottewill, Notes on particle detectors, J. Phys. A **16**, 3905 (1983).
[7] D. Kothawala and T. Padmanabhan, Response of Unruh-DeWitt detector with time-dependent acceleration, Phys. Lett. B **690**, 201 (2010).
[8] J. Doukas, S.-Y. Lin, B. Hu, and R. B. Mann, Unruh effect under non-equilibrium conditions: Oscillatory motion of an Unruh-DeWitt detector, J. High Energy Phys. 11 (2013) 119.
[9] A. Satz, Then again, how often does the Unruh–DeWitt detector click if we switch it carefully?, Classical Quantum Gravity **24**, 1719 (2007).
[10] C. J. Fewster, B. A. Juárez-Aubry, and J. Louko, Waiting for Unruh, Classical Quantum Gravity **33**, 165003 (2016).
[11] R. J. Glauber, Coherent and incoherent states of the radiation field, Phys. Rev. **131**, 2766 (1963).
[12] R. J. Glauber, The quantum theory of optical coherence, Phys. Rev. **130**, 2529 (1963).
[13] E. Bocquillon, V. Freulon, F. D. Parmentier, J.-M. Berroir, B. Plaçais, C. Wahl, J. Rech, T. Jonckheere, T. Martin, C. Grenier *et al.*, Electron quantum optics in ballistic chiral conductors, Ann. Phys. (Amsterdam) **526**, 1 (2014).
[14] D. W. Sciama, P. Candelas, and D. Deutsch, Quantum field theory, horizons and thermodynamics, Adv. Phys. **30**, 327 (1981).

[15] S. Takagi, Vacuum noise and stress induced by uniform acceleration Hawking-Unruh effect in Rindler manifold of arbitrary dimension, Prog. Theor. Phys. Suppl. **88**, 1 (1986).
[16] P. Flandrin, *Time-Frequency/Time-Scale Analysis* (Academic Press, New York, 1998), Vol. 10.
[17] E. Wigner, On the quantum correction for thermodynamic equilibrium, Phys. Rev. **40**, 749 (1932).
[18] S. Haroche and J.-M. Raimond, *Exploring the Quantum: Atoms, Cavities, and Photons* (Oxford University Press, New York, 2006).
[19] D. Ferraro, A. Feller, A. Ghibaudo, E. Thibierge, E. Bocquillon, G. Fève, C. Grenier, and P. Degiovanni, Wigner function approach to single electron coherence in quantum Hall edge channels, Phys. Rev. B **88**, 205303 (2013).
[20] B. Roussel, C. Cabart, G. Fève, E. Thibierge, and P. Degiovanni, Electron quantum optics as quantum signal processing, Phys. Status Solidi B **254**, 1600621 (2017).
[21] B. F. Svaiter and N. F. Svaiter, Inertial and noninertial particle detectors and vacuum fluctuations, Phys. Rev. D **46**, 5267 (1992).
[22] R. F. Streater and A. S. Wightman, *PCT, Spin and Statistics, and All That* (Princeton University Press, Princeton, NJ, 2016).
[23] P. Langlois, Causal particle detectors and topology, Ann. Phys. (Amsterdam) **321**, 2027 (2006).
[24] J. Louko and A. Satz, How often does the Unruh-DeWitt detector click? Regularization by a spatial profile, Classical Quantum Gravity **23**, 6321 (2006).
[25] N. Obadia and M. Milgrom, Unruh effect for general trajectories, Phys. Rev. D **75**, 065006 (2007).
[26] D. Buchholz and J. Schlemmer, Local temperature in curved spacetime, Classical Quantum Gravity **24**, F25 (2007).
[27] D. Buchholz and C. Solveen, Unruh effect and the concept of temperature, Classical Quantum Gravity **30**, 085011 (2013).
[28] C. Barcelo, S. Liberati, S. Sonego, and M. Visser, Minimal conditions for the existence of a Hawking-like flux, Phys. Rev. D **83**, 041501(R) (2011).
[29] L. C. Barbado and M. Visser, Unruh-DeWitt detector event rate for trajectories with time-dependent acceleration, Phys. Rev. D **86**, 084011 (2012).
[30] See Supplemental Material at http://link.aps.org/supplemental/10.1103/PhysRevD.100.045016 for details about singularities in the acceleration, the adiabatic regime and its breakdown, the Wigner function for Fock and coherent excitations, and the approximation schemes.
[31] A. Higuchi, G. E. A. Matsas, and C. B. Peres, Uniformly accelerated finite-time detectors, Phys. Rev. D **48**, 3731 (1993).
[32] L. Sriramkumar and T. Padmanabhan, Finite-time response of inertial and uniformly accelerated Unruh-DeWitt detectors, Classical Quantum Gravity **13**, 2061 (1996).
[33] K. Lochan and T. Padmanabhan, Inertial nonvacuum states viewed from the Rindler frame, Phys. Rev. D **91**, 044002 (2015).
[34] T. Padmanabhan, General covariance, accelerated frames and the particle concept, Astrophys. Space Sci. **83**, 247 (1982).
[35] L. Sriramkumar and T. Padmanabhan, Probes of the vacuum structure of quantum fields in classical backgrounds, Int. J. Mod. Phys. D **11**, 1 (2002).
[36] A. Ashtekar and A. Magnon, Quantum fields in curved space-times, Proc. R. Soc. A **346**, 375 (1975).
[37] R. Haag, *Local Quantum Physics: Fields, Particles, Algebras (Theoretical and Mathematical Physics)* (Springer, New York, 1996).
[38] P. Borgnat, P. Flandrin, P. Honeine, C. Richard, and J. Xiao, Testing stationarity with surrogates: A time-frequency approach, IEEE Trans. Signal Process. **58**, 3459 (2010).
[39] I. Fuentes-Schuller and R. B. Mann, Alice Falls into a Black Hole: Entanglement in Noninertial Frames, Phys. Rev. Lett. **95**, 120404 (2005).
[40] D. Su and T. C. Ralph, Decoherence of the Radiation from an Accelerated Quantum Source, Phys. Rev. X **9**, 011007 (2019).